AN INTEGRAL OPERATOR BASED ADAPTIVE SIGNAL SEPARATION APPROACH

*Xiyuan Hu, Silong Peng**

Institute of Automation
Chinese Academy of Sciences
Beijing 100190, China
{xiyuan.hu, silong.peng}@ia.ac.cn

Wen-Liang Hwang

Institute of Information Science
Academia Sinica
Taipei 11529, Taiwan
whwang@iis.sinica.edu.tw

ABSTRACT

The operator-based signal separation approach uses an adaptive operator to separate a signal into additive subcomponents. And different types of operator can depict different properties of a signal. In this paper, we define a new kind of integral operator which can be derived from the second kind of Fredholm integral equation. Then, we analyze the properties of the proposed integral operator and discuss its relation to the second condition of Intrinsic Mode Function (IMF). To demonstrate the robustness and efficacy of the proposed operator, we incorporate it into the Null Space Pursuit algorithm to separate several multicomponent signals, including a real-life signal.

Index Terms— Integral equation, intrinsic mode function, operator based, Null Space Pursuit (NSP)

1. INTRODUCTION

Recently, many approaches have been proposed to separate a single-channel signal into a mixture of several additive coherent subcomponents [1, 2, 3, 4, 5, 6]. The methods used to separate signals vary because the definitions of subcomponents are different. For example, the subcomponent used in the empirical mode decomposition (EMD) approach [2] is defined as Intrinsic Mode Function (IMF); in the Synchrosqueezed wavelet transform [5, 6], the subcomponent is called the intrinsic mode type function (IMT); and in the operator-based approach [3, 4], each extracted subcomponent is defined as in the null space of the proposed operators.

In the EMD approach, a function $f(t)$ is defined to be an IMF, if it satisfies two conditions [2]: (1) $f(t)$ has exactly one zero-cross point between any two consecutive local extrema; and (2) the local mean of the $f(t)$ should be zero. For the first condition, Sharpley and Vatchev [7] have proved that it equals to the condition that the IMF is a solution of the self-adjoint ODE with the form

$$(Pf')' + Qf = 0, \tag{1}$$

*This work was supported by the Natural Science Foundation of China (61201375,61201050) and the State Key Program of Natural Science Foundation of China (Grant No.61032007).

where P and Q are positive continuously differentiable functions. In the operator-based approach [3], the differential operator with a similar form as in Eq. (1) has been used to extract local narrow band signals. Although the differential operator can characterize the oscillatory property of the signal, it cannot keep the signal's symmetric property well. Furthermore, the differential operator is not robust when the signal is contaminated by noise. The second condition of IMF is used to describe the symmetry of signal [8]. But its explicit definition is still under the veil because the 'local mean' is hard to define accurately. Also, the integral operator, which might similar to the IMF's second condition, has not been assigned an explicit form. The integral operator used in [3] is a simple local mean as $\mathcal{T}(S)(t) = \int_{B_t} S(x)dx$, where B_t is the integral interval which is derived by interpolating from the local extrema of the signal. This kind of operator is not sufficient to annihilate a great number of narrow band signals.

In this paper, we propose a new generalized integral operator with the form

$$\mathcal{T}(S)(t) = \int_{B_t} K(x,t)S(x)dx \tag{2}$$

where $K(x,t)$ is the parameterized integral kernel function and B_t is the integral interval at time t. More specifically, we give an explicit form of the kernel function $K(x,t)$ such that, if we choose a correct integral interval B_t, local narrow band signals can be annihilated by this kind of integral operator. To analyze the properties of the proposed kernel function, we compare it with the differential operator used in [4]. Then, based on the null space pursuit (NSP) algorithm, we implement our adaptive signal separation algorithm using the proposed integral operator. We demonstrate the robustness and efficacy of our proposed algorithm for the noisy and real-life signals in the experimental part.

2. NULL SPACE PURSUIT (NSP) ALGORITHM

The operator-based signal separation approach separates a signal S into U and R such that $U = S - R$ is in the null space of an operator $\mathcal{T}$ [3]. The objective of signal separation in the operator-based approach is to solve the following optimization problem:

$$\hat{R} = \arg\min_{R} \left\{ \|\mathcal{T}(S-R)\|^2 + \lambda \|\mathcal{D}(R)\|^2 \right\}, \tag{3}$$

where R is the residual signal, and $\mathcal{D}$ is a differential operator that regulates R. Minimizing the term $||\mathcal{T}(S-R)||^2$ indicates that $S-R$ is in the null space of the operator $\mathcal{T}$. The main difficulty in applying the operator-based approach to a real-life signal is to determine the correct value of λ, since different λ values can result in different separation results.

To solve the above problem, the NSP algorithm was proposed [4]. The algorithm minimizes the following problem to estimate the signal $\hat{R}$:

$$\hat{R} = \arg\min_{R} \{ ||\mathcal{T}(S-R)||^2 + \lambda(||R||^2 + \gamma||S-R||^2) + F(\mathcal{T}) \}. \tag{4}$$

The first and the second terms of Eq. (4) correspond to the corresponding terms in Eq. (3). The leakage parameter γ in the third term of Eq. (4) determines the amount of $S-U$ to be retained in the null space of $\mathcal{T}$; and the last term $F(\mathcal{T})$ is a Lagrange term for regularizing the parameters of the operator $\mathcal{T}$. When the leakage parameter γ is set to zero, Eq. (4) is reduced to Eq. (3). More important, the parameters λ and γ can be adaptively estimated in the NSP algorithm [4].

3. INTEGRAL OPERATORS FOR SIGNAL SEPARATION

3.1. Integral Operator and its Properties

In the NSP algorithm [4], the differential operator

$$\mathcal{T}_D = d^2/dt^2 + \varpi^2(t) \tag{5}$$

is used to extract the local narrow band signals, where $\varpi(t)$ denotes the instantaneous frequency (**IF**) of the signal. This kind of operator, however, cannot keep the signal's symmetry well because of its small support domain. For instance, consider an input signal as $S(t) = S_1(t) + S_2(t)$ with $S_1(t)$ is a frequency modulated (FM) signal and $S_2(t)$ is a piecewise smooth signal, which are shown in Fig. 1(a), (b) and (c), respectively. Since in the most part of $S_2(t)$, we have $d^2S_2(t)/dt^2 = 0$, the operator in Eq. (5) will not only annihilate the subcomponent $S_1(t)$, but also greatly reduce the energy of subcomponent $S_2(t)$. Thus, in this example, the NSP algorithm cannot extract the desired subcomponent $S_1(t)$ from $S(t)$ because we have $\mathcal{T}_D S(t) \approx 0$.

To overcome the drawbacks of the differential operator, the IMF's second condition which is similar to an integral operation comes into our mind. To define an integral operator that can annihilate a specific kind of signal, we need to find the integral equation that the signal satisfied. Fortunately, the differential equation $d^2S(t)/dt^2 + \varpi^2(t)S(t) = 0$ with

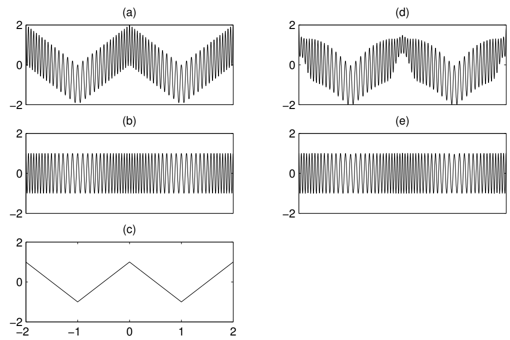

Fig. 1. An example of separating a two component signal. (a, b, and c) the input signal and its two subcomponent, respectively; (d) the extracted subcomponent derived by the NSP [4]; (e) the extracted signal by the proposed algorithm.

boundary values $S(a) = c_1$ and $S(b) = c_2$ can be transformed to the type-II Fredholm integral equation [9]:

$$S(t) = \int_a^b K(x,t)S(x)dx + C(t), \tag{6}$$

where $C(t) = (c_2 - c_1)t/(b-a) + c_1$, and $K(x,t)$ is the kernel function with the form:

$$K(x,t) = \begin{cases} (1-(x-a)/(b-a))\, t\varpi^2(x), & a \le x \le t \\ (1-(t-a)/(b-a))\, x\varpi^2(x), & t \le x \le b \end{cases} \tag{7}$$

Then, considering a signal $S(t)$, we define the integral operator $\mathcal{T}_I$ according to Eq. (6) as

$$\mathcal{T}_I(S)(t) = \int_{B_t} K(x,t)S(x)dx + C(t) - S(t), \tag{8}$$

where B_t is the integral interval.

Although the integral operator in Eq. (8) comes from the differential operator in Eq. (5), their capabilities are quite different. As in Eq. (8), for each point τ, if we choose its neighborhood $B_\tau = [\tau_a, \tau_b]$ with $S(\tau_a) = S(\tau_b) = S(\tau)$, we can have $\mathcal{T}_I(S)(\tau) = \int_{B_\tau} K(x,\tau)S(x)dx = 0$, which reflects the symmetry condition of the input signal. For example, for an FM signal $S(t) = \cos(\phi(t))$ with $\phi'(t) > 0$, τ_a and τ_b can be chosen as $\phi^{-1}(\phi(\tau) - 2\pi)$ and $\phi^{-1}(\phi(\tau) + 2\pi)$, respectively. As shown in Fig. 1(e), the extracted subcomponent is derived by the proposed integral operator defined in Eq. (8). Furthermore, the integral operator is more robust than the differential operator for extracting signals under the noises, which can be seen in the experimental part.

3.2. Integral Operator based Signal Separation

Since the integral operator depends much on the boundary values, the most important drawback of the integral operator

Algorithm 1 NSP Algorithm using Integral Operator

Input signal $\mathbf{s}$, choose a stopping threshold ϵ and the values of λ^0 and γ^0.
Set $j \leftarrow 0$, $\hat{\mathbf{r}}_j \leftarrow 0$, $\lambda^j \leftarrow \lambda^0$ and $\gamma^j \leftarrow \gamma^0$.
repeat
  Estimate the parameters $\varpi(t)$ according to Eq. (13) and compute the integral interval B_t.
  Compute λ^{j+1} according to Eq. (14) using $\mathbf{M}(\lambda^j, \gamma^j, \hat{\mathbf{T}}_j)$.
  Compute $\hat{\mathbf{r}}_{j+1}$ according to Eq. (12) using $\gamma^j, \hat{\mathbf{T}}_j$, and λ^{j+1}.
  Compute γ^{j+1} according to Eq. (15) using $\hat{\mathbf{r}}_{j+1}$ and set $j = j + 1$.
until $\|\hat{\mathbf{r}}_{j+1} - \hat{\mathbf{r}}_j\|^2 < \epsilon$
return Extract mono-component $\hat{\mathbf{u}} = (1 + \gamma^j)(\mathbf{s} - \hat{\mathbf{r}}_j)$ and the residual signal $\hat{\mathbf{r}} = \mathbf{s} - \hat{\mathbf{u}}$.

is to choose a suitable neighborhood, especially when the input signal is a multicomponent signal. In our implementation, we choose an approximate neighborhood B_t according to the estimated **IF** $\hat{\varpi}(t)$ at t; and then, we eliminate the boundary effects by putting the boundary values into the optimization process.

For each point t, the value of $B_t = [a, b]$ is computed by $a = t - 1/\hat{\varpi}(t)$ and $b = t + 1/\hat{\varpi}(t)$. Then, the integral operator defined in Eq. (8) is modified into the following form:

$$\mathcal{T}_I(S)(t) = \int_a^b \left(J(x,t) + K(x,t)\right) S(x)\, dx, \qquad (9)$$

with $J(x,t) = \delta(x-a) - \delta(x-t) + \frac{t-a}{b-a}\delta(x-a)\left(\mathcal{W}_{(b-a)} - \mathcal{I}\right)$ where $\delta(x)$ is the Dirac function with $\delta(t) = 1$ if $t = 0$ and otherwise $\delta(t) = 0$, $\mathcal{W}_{\Delta t}$ denotes the shift operator with $\mathcal{W}_{\Delta t}(S)(t) = S(t + \Delta t)$ and $\mathcal{I}$ is the identity operator; and $K(x,t)$ is defined in Eq. (7). For a given signal $S(t)$, we can use the NSP algorithm to search for $\hat{R}(t)$ by minimizing the equation:

$$\mathcal{F}(R) = \sum_{\tau=1}^{T} \|\mathcal{T}_\tau(S - R)\|^2 + \lambda\left(\|R\|^2 + \gamma\|S - R\|^2\right), \qquad (10)$$

where $\mathcal{T}_\tau$ denotes the integral operator $\mathcal{T}_I$ at time τ.

In discrete representation, we use bold upper case, e.g. $\mathbf{A}$, to represent matrices and bold lower case, e.g. $\mathbf{a}$, to represent vectors. Then, signals $S(t)$ and $R(t)$ can be represented as $\mathbf{s}$ and $\mathbf{r}$, respectively. The integral operator $\mathcal{T}_\tau$ and the second order differential operator $\mathcal{D}_2$ can be represented as $\mathbf{T}_\tau$ and $\mathbf{D}_2$, respectively. Then, Eq. (10) can be rewritten as

$$\mathcal{F}(\mathbf{r}) = \sum_{\tau=1}^{T} \|\mathbf{T}_\tau(\mathbf{s} - \mathbf{r})\|^2 + \lambda\left(\|\mathbf{r}\|^2 + \gamma\|\mathbf{s} - \mathbf{r}\|^2\right). \qquad (11)$$

To optimize the problem in Eq. (11) is quite simple since all the terms are in quadratic form. Therefore, by taking simple calculations, $\hat{\mathbf{r}}$ can be estimated by

$$\hat{\mathbf{r}} = \left(\sum_{\tau=1}^{T} \mathbf{T}_\tau' \mathbf{T}_\tau + (1+\gamma)\lambda\mathbf{I}\right)^{-1} \left(\sum_{\tau=1}^{T} \mathbf{T}_\tau' \mathbf{T}_\tau \mathbf{s} + \lambda\gamma\mathbf{s}\right), \qquad (12)$$

where the prime denotes the transposition of matrix and vector. We use the approach in [10, 11] to estimate the **IF** $\hat{\varpi}(t)$ as

$$\hat{\varpi}^2 = -\left(\mathbf{A}^T\mathbf{A} + \lambda_2 \mathbf{D}_2^T \mathbf{D}_2\right)^{-1} \mathbf{A}^T \mathbf{D}_2(\mathbf{s} - \hat{\mathbf{u}}), \qquad (13)$$

where $\mathbf{A}$ is the diagonal matrix whose diagonal elements equal to $(\mathbf{s} - \hat{\mathbf{u}})$. And following the settings of NSP algorithm [4], the parameters λ and γ in Eq. (11) can be estimated via

$$\hat{\lambda} = \frac{1}{1+\hat{\gamma}} \frac{\mathbf{s}'\mathbf{M}(\lambda, \hat{\gamma}, \hat{\mathbf{T}})'\mathbf{s}}{\mathbf{s}'\mathbf{M}(\lambda, \hat{\gamma}, \hat{\mathbf{T}})'\mathbf{M}(\lambda, \hat{\gamma}, \hat{\mathbf{T}})\mathbf{s}}, \qquad (14)$$

where $\hat{\mathbf{T}} = \sum_{\tau=1}^{T} \mathbf{T}_\tau(\hat{\varpi})'\mathbf{T}_\tau(\hat{\varpi})$ and $\mathbf{M}(\lambda, \hat{\gamma}, \hat{\mathbf{T}}) = (\hat{\mathbf{T}} + (1+\hat{\gamma})\lambda\mathbf{I})^{-1}$; and

$$\hat{\gamma} = \frac{(\mathbf{s} - \hat{\mathbf{r}})'\mathbf{s}}{||\mathbf{s} - \hat{\mathbf{r}}||^2} - 1, \qquad (15)$$

respectively.

Based on equations from (12) to (15), we summarize our integral operator-based signal separation procedure in **Algorithm** 1. This algorithm can be executed M times iteratively to separate a multi-component signal into a sum of M mono-component signals as $\mathbf{s} = \sum_{i=1}^{M} \mathbf{u}_i + \mathbf{r}$, where $\mathbf{r}$ denotes the residual signal.

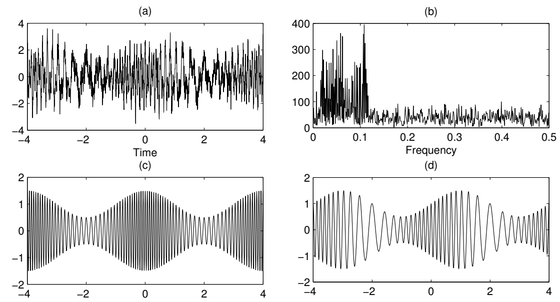

Fig. 2. (a and b) A two-component AM-FM signal $s(t) = s_1(t) + s_2(t) +$ noise and its Fourier spectrum, respectively. Note that the frequency has been normalized from 0 to 0.5. (c and d) the clean subcomponent signal $s_1(t) = 0.5(2 + \cos(0.5\pi t))\cos(20\pi t + 16\sin(0.5\pi t))$ and $s_2(t) = 0.5(2 + \sin(0.5\pi t))\cos(10\pi t + 12\sin(0.5\pi t))$, respectively.

4. EXPERIMENTS AND DISCUSSIONS

In this section, we compare the results of using different signal separation algorithms in experiments on both simulated

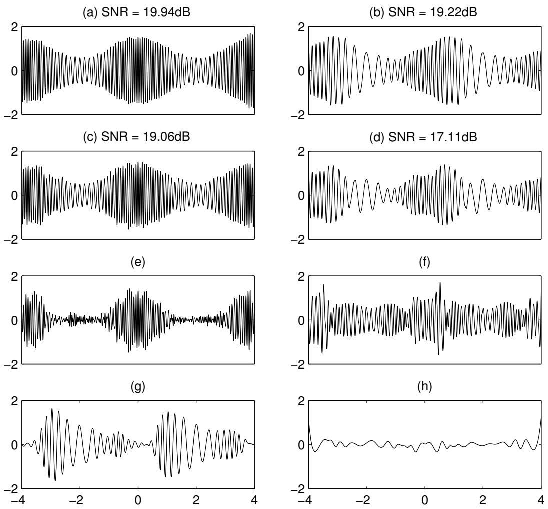

Fig. 3. (a and b) the first and second extracted subcomponents by our proposed algorithm; (c and d) the first and second extracted subcomponents by the SWT [13]; (e to h) the four extracted subcomponents by the EEMD algorithm [12] using the standard variance of real noise.

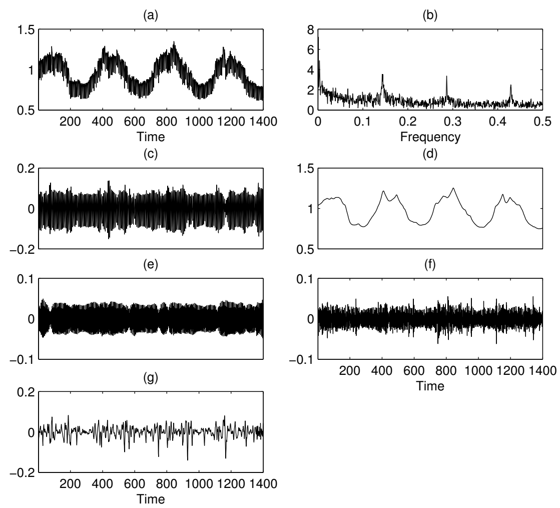

Fig. 4. (a and b) The input signal and its logarithm Fourier spectrum. (c to g) the four extracted subcomponent and the residual signal derived by our proposed algorithm. Noted that, in (b), the frequency has been normalized from 0 to 0.5.

and real-life signals. In the **Simulated Signal** experiment, we test the robustness of our proposed algorithm for separating a two-component AM-FM signal under the noisy case. The input signal and its two subcomponents are shown in Fig. 2(a), (c), and (d), respectively. In this example, since the NSP algorithm [4] can not separate the two signals well, we compare the separation results of the Ensemble EMD (EEMD) [12] and the Synchrosqueezed wavelet transform (SWT) based algorithm [5, 13] in Fig. 3. The first and second row in Fig. 3 show the separation results derived by our algorithm and the SWT based approach, respectively. We can find that both of these two algorithms can extract the two subcomponents correctly. However, the amplitude of the signals extracted by our approach is better than the SWT based approach. Fig. 3 from (e) to (h) show the separation result derived by the EEMD algorithm, from which we can find that EEMD is more like a band-pass filter [14, 15].

In the **Real Example**, we study the signal of Poland's daily electricity consumption from 1990 to 1994 [16]. Since the separation results derived by the EEMD and NSP algorithm can be found in [4, 16], we only show the results derived by our algorithm. Fig. 4(a) and (b) show the input signal and the logarithm of its Fourier spectrum, respectively. Fig. 4(c) to (g) show the first four extracted subcomponents and the residual signal derived by our proposed algorithm. In the extracted subcomponents, each oscillatory subcomponent contains an individual main frequency, which is in accordance with the Fourier spectrum as shown in Fig. 4(b). The first, second, and third extracted subcomponents relate, respectively, to a one-week, one-year, and a half-week cycle, which might correlate with people's working patterns. Note that, the NSP algorithm can not extract the subcomponent with the highest frequency [4].

The appealing feature of the operator-based approach is that the operators can be devised according to the signals, since the different kinds of operator can depict different properties of the signal. In this paper, we propose a new kind of integral operator with an explicit form. Then, we compare the similarity between the integral operator and the second condition of IMF. With the help of Null Space Pursuit algorithm, we implement our proposed operator to separate multicomponent signals. The results of experiments on several simulated and real-life signals demonstrate the efficacy and robustness of the proposed operator for separating multicomponent local narrow band signals.

5. RELATION TO PRIOR WORK

The work presented here has focused on the operator-based adaptive single-channel signal separation algorithm using integral operators. The work by Peng and Hwang [3, 4] considers only differential operators for signal separation. Unlike some time-frequency domain approaches [1, 17], the present study is totally in the time domain and is related to some recent empirical-like approaches [2, 14, 5, 6]. It also analyzes some properties of the new proposed operator and its relation to the IMF's conditions [7, 8, 15], which were not discussed in these earlier studies.

6. REFERENCES

[1] S. Mallat and Z. Zhang, “Matching pursuits with time-frequency dictionaries,” *IEEE Trans. on Signal Processing*, vol. 41, no. 12, pp. 3397–3415, 1993.

[2] N. E. Huang, Z. Shen, S. R. Long, M. L. Wu, H. H. Shih, Q. Zheng, N. C. Yen, C. C. Tung, and H. H. Liu, “The empirical mode decomposition and hilbert spectrum for nonlinear and nonstationary time series analysis,” *Proc. R. Soc. London A*, vol. 454, pp. 903–995, 1998.

[3] Silong Peng and Wen-Liang Hwang, “Adaptive signal decomposition based on local narrow band signals,” *IEEE Transactions on Signal Processing*, vol. 56, no. 7, pp. 2669–2676, 2008.

[4] Silong Peng and Wen-Liang Hwang, “Null space pursuit: An operator-based approach to adaptive signal separation,” *IEEE Transactions on Signal Processing*, vol. 58, no. 5, pp. 2475–2483, 2010.

[5] Ingrid Daubechies, Jianfeng Lu, and Hau-Tieng Wu, “Synchrosqueezed wavelet transforms: An empirical mode decomposition-like tool,” *Applied and Computational Harmonic Analysis*, vol. 30, no. 2, pp. 243–261, 2011.

[6] S. Meignen, T. Oberlin, and S. McLaughlin, “A new algorithm for multicomponent signals analysis based on synchrosqueezing: with an application to signal sampling and denoising,” *IEEE Transactions on Signal Processing*, vol. 60, no. 11, pp. 5787–5798, 2012.

[7] Robert C. Sharpley and Vessenlin Vatchev, “Analysis of the intrinsic mode functions,” *Constructive Approximation*, vol. 24, no. 1, pp. 17–47, 2006.

[8] Q. Chen, N. E. Huang, S. Riemenschneider, and Y. Xu, “A B-spline approach for empirical mode decompositions,” *Advances in Computational Mathematics*, vol. 24, no. 1, pp. 171–195, 2006.

[9] Kôsaku Yosida, *Lectures on differential and integral equations*, Interscience Publishers, New York, 1991.

[10] X. Hu, S. Peng, and W.-L. Hwang, “Estimation of instantaneous frequency parameters of the operator-based signal separation method,” *Advances in Adaptive Data Analysis*, vol. 1, no. 4, pp. 573–586, 2009.

[11] X. Hu, S. Peng, and W.-L. Hwang, “Multicomponent AM-FM signal separation and demodulation with null space pursuit,” *Signal, Image and Video Processing*, pp. 1–10, 2012.

[12] Z. Wu, N. E. Huang, and X. Chen, “The multi-dimensional ensemble empirical mode decomposition method,” *Advances in Adaptive Data Analysis*, vol. 1, no. 3, pp. 339–372, 2009.

[13] E. Brevdo, N. S. Fuĉkar, G. Thakur, and H.-T. Wu, “The synchrosqueezing algorithm: a robust analysis tool for signals with time-varying spectrum,” *arXiv:1105.0010*, pp. 1–29, 2011.

[14] Gabriel Rilling, Patrick Flandrin, and Paulo Goncalves, “On empirical mode decomposition and its algorithms,” in *IEEE-EURASIP Workshop on Nonlinear Signal and Image Processing*, 2003.

[15] Gabriel Rilling and Patrick Flandrin, “One or two frequencies? the empirical mode decomposition answers,” *IEEE Transactions on Signal Processing*, vol. 56, no. 1, pp. 85–95, 2008.

[16] Q. Xie, B. Xuan, S. Peng, J. Li, W. Xu, and H. Han, “Bandwidth empirical mode decomposition and its application,” *International Journal of Wavelets, Multiresolution and Information Processing*, vol. 6, no. 6, pp. 777–798, 2008.

[17] R. Carmona, W. L. Hwang, and B. Torresani, “Multiridge detection and time-frequency reconstruction,” *IEEE Trans.on Signal Processing*, vol. 47, no. 2, pp. 480–492, 1999.